High yield detritylation of surface-attached nucleosides with photoacid generated in an overlying solid film: roles of translational diffusion and scavenging†

Peter B. Garland*[a] and Pawel J. Serafinowski[b]

Received 31st July 2008, Accepted 28th October 2008
First published as an Advance Article on the web 28th November 2008
DOI: 10.1039/b813319k

Conventional solid-phase oligonucleotide synthesis overcomes the reversibility of acid-dependent detritylation by washing away the released dimethoxytrityl cations (DMT^+) with acid. This option is unavailable if the acid is photogenerated in an overlying solid film, as in the photolithographic fabrication of oligonucleotide arrays on planar surfaces. To overcome the resulting reversibility problem we developed methods of achieving ≥98% detritylation of glass-attached 5′-*O*-DMT-thymidine, a model for 5′-*O*-DMT-protected oligonucleotides, by the photogeneration of trichloroacetic acid in a solid film. Enhanced intrafilm diffusion, insufficient to degrade the photolithographic resolution but enabling DMT^+ to move from its plane of release into the overlying photoacid-generating film, increased detritylation from ≤30% to ≥98%. Inclusion of an intrafilm carbocation scavenger such as a triarylsilane hydride converted the detritylation into a time-dependent irreversible process proceeding to ≥99% detritylation within 60 s following brief photoacid generation. Light sensitivity is high, exceeding direct photodeprotection methods by 15–100 fold.

Introduction

The early fabrication[1,2] of oligonucleotide microarrays by synthesis *in situ* was on planar glass surfaces, using the same chemistry as for much larger scale conventional solid phase oligonucleotide synthesis[3] on glass or plastic beads. Physical barriers directed critical reagent solutions to specified array elements. Array density was low, with individual elements of mm dimensions. Much higher array densities were obtained by the use of a photocleavable blocking group in place of DMT,[4] and exposure of the array surface to patterned illumination to define the array elements and their base sequences.[5]

An alternative photolithographic approach retained DMT as the protecting group, and used patterned illumination of a solid polymer film containing a photoacid generator applied to the array surface for the detritylation step.[6,7] The film prevents diffusion of the photoacid from illuminated to non-illuminated array elements, but also prevents the diffusion of DMT^+ away from its site of formation. Because acid induced detritylation is reversible it proceeds no further than the equilibrium position with a given acid activity.[8] The need for >98% completion is not met unless the photoacid is strong, but this causes depurination.[9]

We set out to resolve, in solid films, the conflict between the need for virtually complete detritylation and the avoidance of photoacid-induced depurination. Our solution is described in Scheme 1. It depends on the removal of DMT^+, either by diffusion or scavenging.

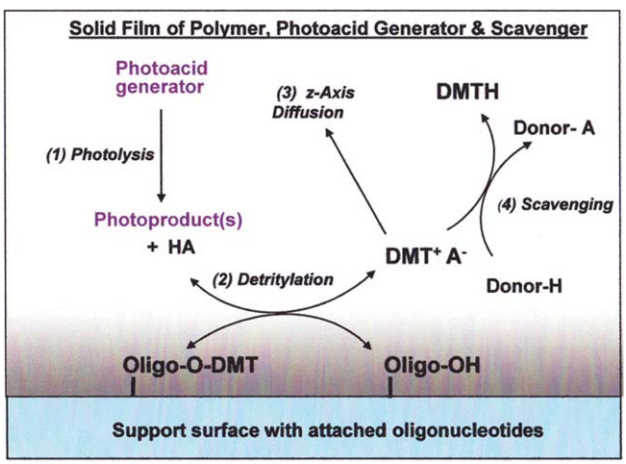

Scheme 1 Vertical section through a photoacid generating film and its solid support. Shading of the film region adjacent to the support surface represents the layer of attached oligonucleotides, a thin virtual compartment communicating by diffusion with the rest of the film. Numbered processes 1 and 4 are irreversible, whereas 2 and 3 are reversible, reaching equilibrium in a few s in the case of 2 but very much longer with 3, depending on intrafilm viscosity and film thickness.

Previous estimates[10] of detritylation efficiency for photoacids in solid films depended on the synthetic yield of oligonucleotides: in its place we have used *in situ* spectrophotometric measurements of the intrafilm photoacid-induced release of DMT^+ from DMT-T covalently attached by 3′-*O* linkage to a planar glass surface. The area densities of surface-attached DMT-T were high, 5–15 fold higher than the 40 pmol cm^{-2} normally used for oligonucleotides

[a]*Section of Molecular Carcinogenesis, The Institute of Cancer Research, Sutton, Surrey, UK SM2 5NG. E-mail: peter@garland.org.uk*
[b]*Cancer Research UK Centre for Cancer Therapeutics, The Institute of Cancer Research, Sutton, Surrey, UK SM2 5NG. E-mail: Pawel.serafinowski@icr.ac.uk*

† Electronic supplementary information (ESI) available: Further information on experimental; detritylation equilibrium equations; computer simulation details; kinetics of DMT^+ scavenging; diffusion and film composition. See DOI: 10.1039/b813319k

in arrays.[1] These high densities were chosen to improve the accuracy of detritylation determinations. Their drawback was a lower detritylation extent at equilibrium with photoacid.

Results

Computer modeling (ESI†)

Detritylation equilibrium. The ratio of tritylated to non-tritylated nucleotide concentrations in equilibrium with an acid is given by:

$$\frac{[\text{DMT-}O\text{ - oligonucleotide}]}{[\text{HO-oligonucleotide}]} = \frac{[\text{DMT}^+\text{A}^-]}{[\text{HA}]K_{eq}} \quad (1)$$

where K_{eq} is the apparent equilibrium constant, DMT^+A^- is the ion pair of DMT^+ carbocation and acid anion, and HA is the total acid which is assumed to be in many-fold excess over the other reactants. Concentrations are used in place of activities. Detritylation approaches completion when the left hand term in equation (1) approaches zero. This relationship gives three independent options for increasing the extent of detritylation at equilibrium: increase the strength of the acid; replace DMT with a more acid-sensitive group; remove DMT^+ from its site of origin.

The first of these three options is limited: K_{eq} as defined by equation (1) increases with acid strength, but so does depurination risk. The second suffers from loss of a reagent used in many well characterized and commercially available compounds; the required increase in acid-sensitivity might also be accompanied by instability.[11] The third option, removing DMT^+, has two possibilities for realisation: (a) provide for intrafilm diffusion of DMT^+ away from its site of formation on the surface of the array support, and (b) include within the film a scavenging agent for DMT^+.

Fig. 1 shows the calculated effect on the detritylation equilibrium of reducing the activity of DMT^+ by 1–50 fold. The effects are considerable: a 20-fold reduction from 1.0 to 0.05 can increase detritylation from <80% to >98%.

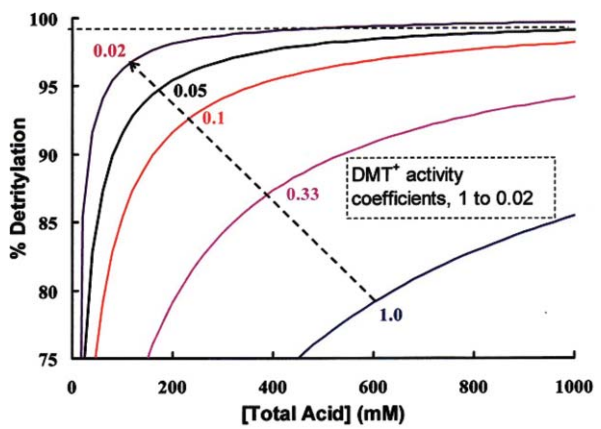

Fig. 1 Calculated effects of DMT^+ removal on the extent of detritylation at equilibrium. The number by each curve is an activity coefficient applied to $[DMT^+A^-]$ in equation (1). The value for K_{eq} was 0.05, and the initial concentration of surface-attached DMT-groups of 25 mM was calculated from a surface density of 250 pmol cm^{-2} occupying a thickness of 10 nm. The value used for K_{eq} is from measurements of detritylation by photogenerated TCA for DMT-T distributed throughout a solid film of photoacid generator.[8]

DMT^+ diffusion. A film overlaying a layer of oligonucleotides covalently attached to a planar support surface can be regarded as two compartments: the film, typically several hundred nm thick, and the surface-attached oligonucleotide layer which has a depth of only 10–20 nm or less depending on chain length. Diffusion of DMT^+A^- from the oligonucleotide layer into the overlying film is therefore a possible means of enhancing detritylation.

One-dimensional molecular diffusion can be simulated by using equidistant jumps $\pm d$ in length occurring at constant frequency. The Einstein-Smoluchowski equation[12] applies:

$$< d^2 > = 2Dt \quad (2)$$

where $< d^2 >$ is the mean square of the distance diffused, D the diffusion coefficient and t the jump period.

Fig. 2 shows results from simulating the effects of diffusion on the intrafilm profile of DMT^+ concentration along the z-axis. DMT^+ is released into the oligonucleotide layer at the underlying support surface, and its diffusion into the overlying film generates new concentration profiles. The calculated concentration of DMT^+ in the thin surface zone of attached oligonucleotide fell by over 10-fold after 10^4 diffusional jumps. This fall would significantly increase detritylation (Fig. 1).

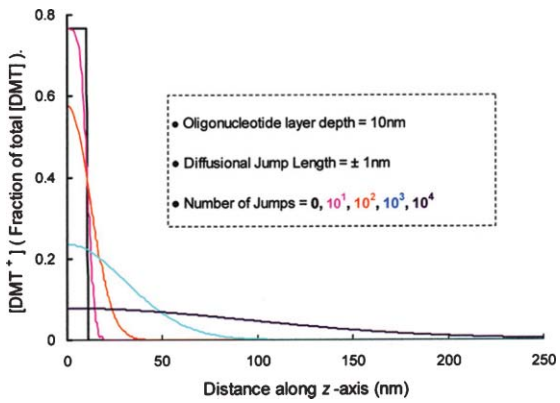

Fig. 2 Calculated changes of intrafilm concentration profiles of DMT^+ in the z-axis due to diffusion from an immobile 10 nm thick layer of 5′-*O*-DMT-oligonucleotide following photoacid generation. At zero time all DMT^+ is within the oligonucleotide layer. Initial values used for calculations were $K_{eq} = 0.1$, [HA] = 250 mM, and [5′-*O*-DMT-oligonucleotide] = 10 mM (corresponding to 100 pmol cm^{-2} before photoacid generation). Detritylation after 0, 10^1, 10^2, 10^3 and 10^4 diffusional jumps was 76, 79, 83, 92 and 97% respectively.

But enhancement of diffusion to achieve greater detritylation raises a question: would comparable rates of photoacid diffusion in the plane of the film cause loss of photolithographic resolution? Diffusion constants are only weakly dependent on molecular weight. We carried out simulations of TCA diffusion across the boundary between illuminated and non-illuminated areas, again using a repetitive jump model. After 10^4 jumps of ± 1 nm significant concentrations of photoacid did not extend more than 200–250 nm beyond the light/dark boundary (ESI†), a distance unlikely to compromise resolution of 10 × 10 μm array elements.

Intrafilm diffusion and film composition

Surface loss of TCA. Both increased intrafilm acidity (sensed by BG, a pH sensitive dye) and DMT^+ formation following photoacid generation can be measured spectrophotometrically *in situ*.[8] In thin films (<100 nm) of ester **2** as the film-forming component these absorbance changes slowly reverse with time (Fig. 3). Reversal was not seen if a cover slip overlaid the film surface, or the if the film thickness was a few-fold greater.

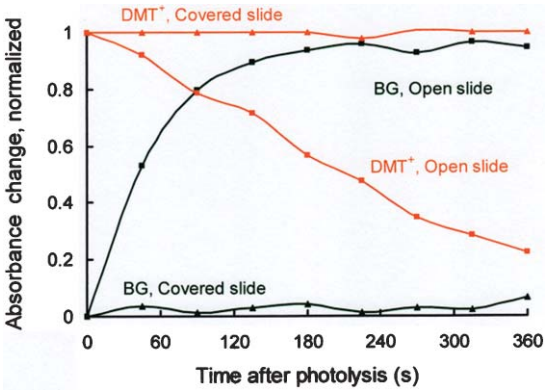

Fig. 3 Time-dependent absorption changes following photolysis (15 s at 32 mW cm^{-2}) of a thin (80–90 nm) film of ester **2** (18 nmol cm^{-2}) containing DMT-T (0.2 nm cm^{-2}) and BG (0.2 nmol cm^{-2}), measured at 510 nm (DMT^+) and 640 nm (BG). Absorbance values are normalized to those immediately prior to photolysis for BG, and 10 s after photolysis for DMT^+.

Solid TCA vaporizes, and its continued loss from a film is dependent on intrafilm diffusion to reach the air/film interface The intrafilm concentration of DMT^+ is not a linear representation of intrafilm TCA concentration, but its time-dependent decay as seen in Fig. 3 may be compared with computer simulated data (ESI†) to obtain an approximate value of *ca.* 50 nm^2 s^{-1} for D_{TCA}, the intrafilm diffusion coefficient for TCA in films of ester **2**. Decays as in Fig. 3 were not observed if the film contained PMS[4] at weight ratios to ester **2** ranging from 1:1 to 4:1, where we estimated $D_{TCA} < 0.1$ nm^2 s^{-1}. These values are semi-quantitative, but the large differences between them do indicate differences in intrafilm viscosity as experienced by TCA. Diffusion coefficients show only a weak dependence on mol wt, and we anticipate that similar values would apply to the ion pair DMT^+A^-.

Patterned photoactivation. Diffusion in the x or y axes in a plane can be measured by a patterned photoactivation method.[13,14] Diffusion is observed as time-dependent decay of the pattern.

Using photolysis through a Rhonchi ruling[15] with 50 line pairs per mm contacted with the surface of a film of ester **2** containing BG, we generated a pattern of alternating green and colorless lines (Fig. 4). Unfortunately the relatively large width of the lines made relaxation of the pattern too slow for useful spectrophotometric measurement on films where the ruling was left in place following photolysis (ESI†). But it was useful to demonstrate the imaging potential of such films at a resolution appropriate for array fabrication.

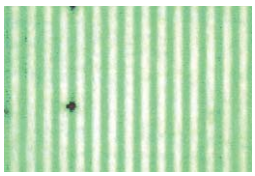

Fig. 4 Patterned photo-acidification of a film of **2**. The film was made by rapidly dip-coating a 25 × 6 mm piece of glass slide with a solution of 2% (w/v) ester **2** (*ca.* 40 mM) and 5 mM BG and allowing it to dry. Film was removed from one surface with solvent. The remaining film was illuminated (365 nm, 20 s, 40 mW cm^{-2}) through a contacted Ronchi ruling of 50 line pairs mm^{-1}, then examined by transmitted white light with a digital microscope. The white and green bands, 10 μm wide, are the exposed and non-exposed areas respectively, corresponding to protonated and non-protonated BG.

Detritylation of surface-attached DMT-T

We used 5′-*O*-dimethoxytritylthymidine as a model for acid-induced oligonucleotide detritylation. Rates and equilibria of detritylation may vary between nucleosides, nucleotides or oligonucleotides. But the reaction itself, in the solid environment of a diffusion-restricting photoacid-generating film, is essentially unchanged, as is the task of achieving ≥98% completion of detritylation.

Extent. Using glass slides with surface-attached DMT-T (120–700 pmol cm^{-2}) and coated with thin films (0.3–1.5 μm) of ester **2** without added polymers, we measured detritylation as shown by the formation of DMT^+ in response to photolytic illumination (typically 20–25 mW cm^{-2} for 30 s).[16] To determine the amount of DMT-T remaining on the glass the exposed film was removed with solvent, replaced with a fresh film and photolysed as before. Under these conditions little if any DMT^+ was detected after photolysis of the second film. We concluded that the first photolysis had achieved ≥98% detritylation. These high levels of detritylation of surface-attached DMT-T were independent of the attachment chemistry.

Kinetics. We had previously observed[8] that release of DMT^+ from DMT-T incorporated within a film of ester **2**, with or without added PMS, remained approximately in phase with repeated short periods of illumination, equilibrating with photoacid within 5–10 s after each period.

Different kinetics were observed when using surface-attached DMT-T. Fig. 5 shows the time course of detritylation following a single brief photolytic exposure. The initial post-photolysis height of the 510 nm absorbance peak corresponded to *ca.* 40% conversion of DMT-T to DMT^+. Thereafter the peak slowly grew in height to reach a plateau corresponding to >90% conversion. In this experiment the area densities of photoacid and initial DMT-T were respectively 14.6 and 0.4 nmol cm^{-1}. The acid is distributed throughout the 200 nm thick film, whereas DMT-T is restricted to the surface where it forms a layer of local concentration comparable to that of photoacid. The post-illumination progress of detritylation could depend on diffusion of acid from the overlying film to replace that consumed in the DMT-T layer at the glass surface, and of DMT^+ into the film. DMT^+ movement is the more important in this experiment because without it high levels of detritylation could not be achieved by TCA alone.[8]

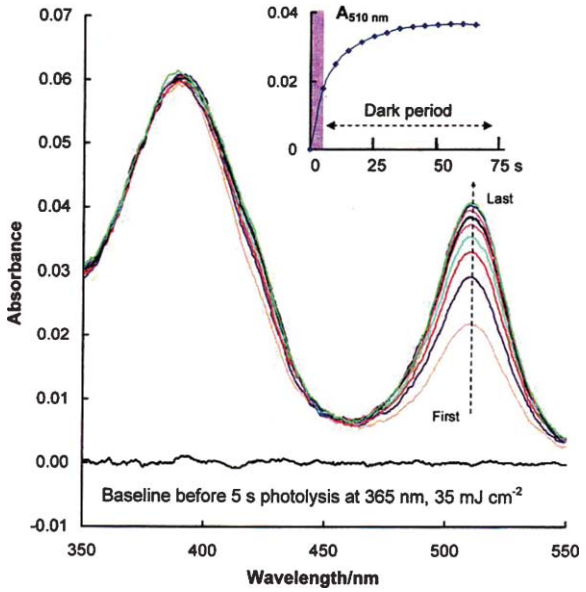

Fig. 5 Kinetics of detritylation by a 200 nm thick film of ester **2** coating a glass slide surface carrying DMT-T at *ca.* 400 pmol cm^{-2}. Photolysis (365 nm, 5 s, 165 mJ cm^{-2}) was immediately followed by measurement of absorbance spectra at 5 s intervals. The peaks at 510 nm and 385 nm are due to DMT^+ ($\varepsilon_{mM} \approx 80$ mM^{-1} cm^{-1}) and the substituted 2-nitrosobenzophenone photoproduct ($\varepsilon_{mM} \approx 4.1$ mM^{-1} cm^{-1}). The anticipated absorbance at 510 nm for a DMT^+ density of 400 pmol cm^{-2} is 0.032, superimposed on a baseline increase due to the nitroso-photoproduct of **2**. The baseline noise is that of a CCD detector.

Intrafilm polymer. Detritylation of surface-attached DMT-T caused by photolysis of overlying ester **2** films containing an equal or greater amount of PMS[17] gave <30% detritylation, even though photolysis was continued to give similar intrafilm TCA concentrations to those used in the absence of polymer. A protracted dark phase of detritylation as in Fig. 5 was not detected. Parallel experiments with the incorporated pH indicator BG showed that the presence of an appropriate polymer (*i.e.* lacking electronegative heteroatoms[8]) did not lower proton activity at comparable intrafilm TCA concentrations. Our results for the extent and kinetics of detritylation for surface-attached DMT-T differ markedly from those[8] for DMT-T incorporated within the volume of the photoacid generating film. They are consistent with the diffusional model used for Fig. 2 and visualized in Scheme 1.

Plasticizers. So-called plasticizers[18] incorporated within solid polymers lower intrafilm viscosity and increase thermoplasticity by reducing binding between polymer molecules. We screened a range of 16 plasticizers, all lacking electronegative heteroatoms to avoid weakening of TCA,[8] and containing aryl groups in anticipation that they would confer compatibility with polystyrene-based polymers (ESI†). Further selection criteria were high solubility in DCM and no effect on the film-forming ability of solutions of the host polymer (PMS) at plasticizer to polymer ratios ≤1.0 by weight. Triphenylmethane (TPM) was the most promising: unlike the other candidates it formed an optically clear solid film when cast from DCM solution without added polymer.

Table 1 Reactivity of DMT^+ with carbocation scavengers in solution

Reagent	2nd order rate constant[a] (M^{-1} s^{-1})
Tri-*n*-butyltinhydride	1.6×10^3
Triphenyltinhydride (TPTH)	8.7×10^1
Tris(trimethylsilyl)silane	1.9×10^1
Poly(carbomethylsilane)[b]	4.3×10^{-1}
Tetramethyldisiloxane[c]	1.6×10^{-1}
Bis(4-methoxyphenyl)phenylsilane	1.1×10^{-1}
(4-Methoxyphenyl)diphenylsilane (MPDPS)	1.0×10^{-1}
5-Methoxyindole	8.8×10^{-2}
Triethylsilane	5.0×10^{-2}
Poly(methylhydrosiloxane)[d]	2.5×10^{-2}
Triphenylsilane (TPS)	1.3×10^{-2}
Indole	1.2×10^{-2}
Tri-*n*-propylsilane	6.0×10^{-3}
Pyrrole	4.0×10^{-3}
Diphenylsilane	3.3×10^{-3}
Phenylsilane	$<10^{-4}$
Triethoxysilane	$<10^{-4}$
Tri-isopropylsilane	$<10^{-4}$

Notes:[a] The values in the Table for each compound are the averages for at least 3 observations which were consistent to within a few %. In view of the million-fold range of rate constants, no attempt was made to calculate standard deviations. [b] Polymer, average mol wt 2,000 or 900 Da. The repeating subunit is–CH_2-SiH(CH_3)–. [c] Two silylhydride groups per molecule. [d] Oligomer, average mol wt 390 Da, with an average of three silylhydride groups per molecule. All measurements were made spectrophotometrically in 3.2 mL of DCM containing DMT-T (6–10 μM) and TCA (0.1–0.15 M) followed by a few μL of scavenger solution at a concentration that gave suitable rates of absorbance change at 505 nm for absorption measurements over 30–180 s.

Scavenging agents for DMT^+

Potential scavengers. Scavengers of DMT^+ have been included in both solution phase[19] and conventional solid-phase synthesis.[20] In the latter case the scavenger was in the acidic detritylating solution.

We examined the performance of compounds from four classes of candidates: pyrroles, indoles, trialkyl- or triarylsilanes and trialkyl- or triaryltin hydrides. The first two classes react by electrophilic substitution with DMT^+, the latter two by hydride transfer. We extended the range of triarylsilanes by synthesizing (4-methoxyphenyl)-diphenylsilane and bis(4-methoxyphenyl)-phenylsilane as described under Experimental.

The reactivity of the candidate scavengers with DMT^+ in solution provided a simple first screen (Table 1). In all cases the scavenger was present in a several- to many-fold excess over DMT-T. The decay of acid-generated DMT^+ concentrations on addition of scavengers followed pseudo-first order kinetics. The calculated second-order reaction rate constants varied >10^6-fold with scavenger structure. The most reactive were tri-*n*-butyltinhydride and triphenyltinhydride.

Performance. When tested in solid films (Fig. 6) the rates of DMT^+ reaction with TPS or MPDPS followed first order kinetics, in keeping with the excess of scavenger over DMT^+. The reaction of TPTH with DMT^+ differed: despite a very fast initial rate *ca.* 10% of the DMT^+ remained unreacted. This unreactive fraction may represent scavenger-less microdomains of DMT^+. The inclusion of TPM (*ca.* 10% by weight) as a plasticizer in TPTH-containing films resulted in ≥98% removal

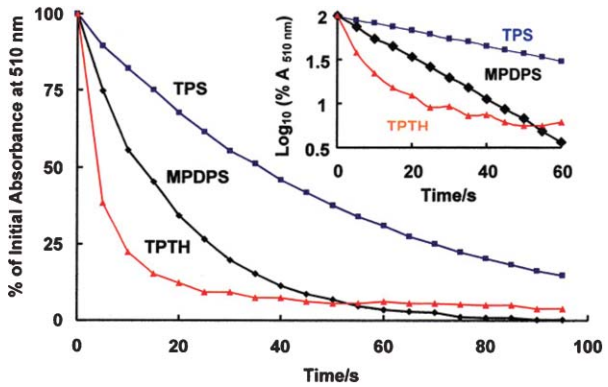

Fig. 6 Reaction kinetics of hydride donors with DMT^+ in a solid film. The inserted graph is semilogarithmic. Films were cast from a DCM solution, 1 mL of which contained 0.75 mg each of ester **2** and PMS, 100 nmol of DMT-T, and one of TPS (0.75 mg) or DMTPS (0.75 mg) or TPTH (0.1 mg). Photolysis (250–320 mJ cm^{-2}) generated TCA to release DMT^+, measured at 510 nm from 5 s onwards after photolysis.

of DMT^+. The less-reactive scavengers TPS and MPDPS are required at several-fold higher concentrations than TPTH, and may themselves act as plasticizers in achieving >98% removal of DMT^+.

We explored incomplete access of scavengers to DMT^+ within films, of poly(carbomethylsilane)[21] acting as both scavenger and film-forming polymer. Ester **2** and DMT-T were included in the films, and DMT^+ removal was measured following brief but intense photolysis to generate TCA (Fig. 7). Reaction kinetics were biphasic, and incomplete. Inclusion of TPM (10% by weight) increased the rate of DMT^+ scavenging by 3–5 fold, and changed the complex kinetics towards a single monotonic decay. The rates were *ca.* two-fold greater with poly(carbomethylsilane) of lower molecular weight.

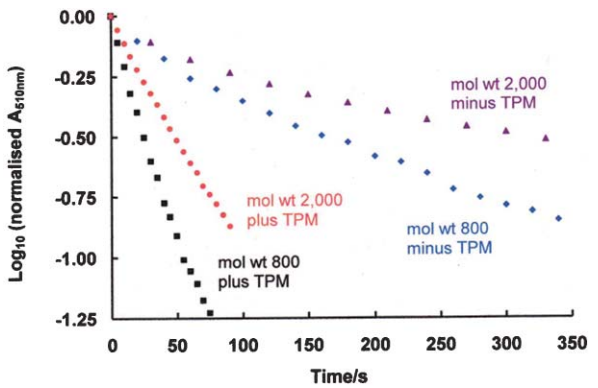

Fig. 7 Scavenging of DMT^+ in solid films of poly(carbomethylsilane) and the effects of added plasticizer. Average mol wt of the polymer sample was either 800 or 2000 Da. Films were cast from a DCM solution, 1 mL of which contained poly(carbomethylsilane) (12 mg), ester **2** (3 mg), and DMT-T (24 nmol) with or without triphenylmethane (1.7 mg). Photolysis and timing of absorbance measurements were as in Fig. 6.

Reaction product(s). Reaction of hydride donors with DMT^+ is irreversible, the C-H bond being stronger than the Si-H or Sn-H bonds.[22] The reaction can be written as:

$$DMT^+A^- + Ar_3SiH = DMTH + Ar_3SiA \quad (3)$$

We identified DMTH (*i.e.* 4,4′-(phenylmethylene)-bismethoxybenzene)) and Ar_3SiA (trisilanetrichloroacetate) as products of the reaction of triphenylsilane in solution with DMT^+ generated from DMT-T with TCA. We found no evidence of 5′-*O*-triphenylsilylthymidine formation.

Pyrrole, indole and 5-methoxyindole were reactive with the DMT^+ in films but there were complex changes in the UV-vis absorbance spectra. Following photolysis the films were not easily washed from the glass slide with solvents. These changes, not seen in solutions where acid was provided by addition rather than photolysis, may be due to photo-induced polymerization of ring systems.

Intrafilm scavenging for surface-attached DMT-T. Experiments were with slides carrying DMT-T at a surface density of *ca.* 400 pmol cm^{-1}. Any DMT-T remaining after the irradiation of a slide coated with a film of ester **2** with added polymer and scavenger was measured by removing the spent film and replacing it with a second film of ester **2** alone before a second irradiation (see Experimental). For example, part of a slide with surface attached DMT-T was coated with a first film composed of PMS, ester **2** and the scavenger MPDPS (1:1:1 by weight), and then briefly photolysed (60 mJ cm^{-2}). The film was removed 60 s later with dichloromethane and then replaced by a second film consisting of ester **2** alone, before a second photolysis (180 mJ cm^{-2}). Spectrophotometric scans of the film following the second photolysis would have detected, at a sensitivity of ± 1.25 pmol cm^{-2}, any DMT^+ originating from surface-attached DMT-T that had escaped detritylation by the first exposure to photoacid. None was detected: thus the first illumination when the film contained a scavenger had been sufficient to remove >99% of DMT-groups within 60 s.

The high surface densities of DMT-T and spectrophotometric sensitivity for DMT^+ required for these experiments are unusual, but without them detritylation values of 98–99% could not have been differentiated from lower ones such as 95–97%. On the other hand the high initial concentration of DMT-T makes it more difficult to achieve high percentage detritylation at equilibrium.

Film composition and detritylation of surface-attached DMT-T

Intrafilm viscosity. Table 2 summarizes the extent of detritylation of surface-attached DMT-T following photolysis of overlying films of ester **2** with or without added PMS or plasticizer TPS. Major observations are that (i) photolysis of ester **2** films supports extensive detritylation, up to at least 98%, (ii) inclusion of PMS reduces detritylation to a maximum of 30%, and (iii) this effect of PMS is overcome by further inclusion of a plasticizer. These observations are consistent with lowered intrafilm viscosity being a cause of higher levels of detritylation.

For comparison we include in Table 2 results for films of ester **2** with incorporated DMT-T,[8] where no amount of diffusion allows DMT^+ to escape from proximity to detritylated thymidine. In those conditions only incomplete detritylation of 70–80% was achieved despite photoacid generation for 3–4 photolytic half-lives.

Table 2 Characteristics of detritylation of DMT-T by photogenerated TCA in solid films[a,b]

Property or process	DMT-T distributed in film		DMT-T attached to glass support		
Film composition[b]	PAG alone	PAG + PMS	PAG alone	PAG + PMS	PAG + PMS + TPM
D_{TCA} ($nm^2\ s^{-1}$)[c]	*ca.* 50	< 0.1	*ca.* 50	< 0.1	100–200
Detritylation[d,e]	Tracks photoacid generation		Plus dark phase[f]	No dark phase	Plus dark phase[f]
Extent of detritylation[g]	70–80%	→	≥ 98%	≤ 30%	≥ 98%
Second detritylation step[h]	Not applicable	→	≤ 2%	≥ 30%	≤ 2%

Notes:[a] Detritylation experiments at ambient temperature (20–23 °C), 1–1.5 μm thick films were made by spread-coating. Ester **2** was used throughout. Casting solutions were in DCM with 2% solids by weight. Ratios by weight were 1:4 for PAG:PMS and 1:4:0.5 for PAG:PMS TPM. For DMT-T attached to glass the surface density was 200–700 pmol cm^{-2}. [b] The values given for % detritylation and diffusion coefficients are for ranges identified by at least three separate experiments for each set of conditions. [c] Diffusion coefficients for TCA were calculated from separate experiments, from T_{half} for decay of BG protonation following photolytic illumination at 365 nm, as shown in Fig. 3 with thin films and also the thicker films (0.5 μm) of PAG + PMS + plasticizer (TPM). [d] As determined by DMT^+ accumulation, measured by absorbance changes at 510 nm. [e] Following exposure at 365 nm, 60–100 mJ cm^{-2} in 5 sec. [f] Continued detritylation after cessation of photoacid generation, as in Fig. 5. [g] Photolysis at 300–400 J cm^{-2}, and exposure plus post-exposure time of 100s. % Detritylation calculated either by reference to pre-photolysis BG or PAG concentration as internal standards for DMT-T incorporated within films, or to the total DMT^+ released from surface-attached DMT-T by repeated exposure to photoacid or elution with TCA solution. Relatively high incident energies were used to minimize any variations in photoacid formation. [h] Following removal by solvent of the film used for the first detritylation step, and then repeating film casting with ester **2** alone followed by illumination as a second detritylation step to detect remaining DMT-T.

Discussion

Computer simulations

Analytical solutions to diffusion equations are complex, but digital simulations are not. We found it instructive, as in Fig. 2, to simulate some of the situations involving diffusion, detritylation and scavenging (see ESI†).

Solid films, polymers, and plasticizers. These topics are interrelated. Solid films lower intrafilm diffusion rates, with two outcomes: bimolecular reactions become diffusion-limited and movement of reaction products away from a localized site of production is impaired. These effects are not marked in solid films of monomeric photoacid generators, and it was fortunate that our preferred class, substituted 2-nitrobenzyl esters of TCA, formed optically clear and uniform films when cast from solution. But inclusion of polymer may be required to provide a more adjustable and less expensive solid environment.

The inclusion of polymers brings potential complications. Diffusion of small molecules in a solid film of linear polymers involves thermal movement of polymer chains to create holes ("free volumes") into which adjacent small molecules may jump.[23] The rates of hole formation are greater at the ends of polymer chains then at their central regions, creating locally different diffusion rates. Polymers can immobilize and isolate smaller molecules that can be trapped between the rigid segments of polymers. Furthermore, supra-molecular microdomains may arise by phase-separation of low molecular weight compounds within a polymer matrix. The inclusion of plasticizers loosens the polymer structure and diminishes the diffusional isolation of smaller molecules within the film.

A further complication arises if components of the photoacid-generating film segregate into microdomains. This cannot occur if the film is composed solely of PAG, as with film-forming substituted 2-nitrobenzyl esters of TCA.[8] Such films have relatively low internal viscosity and included molecules of low molecular weight, such as photosensitizers or scavengers, are less likely to form diffusionally isolated domains.

The role of intrafilm diffusion in increasing the detritylation of surface-attached compound overlaid by a photoacid-generating solid film has not been previously reported, although diffusional enhancement may have unknowingly occurred in experimental protocols using post-exposure heating either with[7] or without[6] chemical amplification of the photoacid. High intrafilm concentrations of reagents for chemical amplification[7,24] or photosensitization[25] may also act as plasticizers.

Scavengers. Removal of DMT^+ by carbocation scavengers has the attraction of converting detritylation following photoacid generation into a time-dependent irreversible process. But microdomain formation is possible, such that not all DMT^+ is accessed by the scavenger. Examples of restricted removal of DMT^+ by scavengers are illustrated in Fig. 6 and 7, as is the ability of added plasticizers to overcome them.

Triarylsilanes have desirable properties for intrafilm scavengers, namely no interference with film formation, no unwanted photochemical reactions, detritylation of DMT-T to below detection limits, monophasic DMT^+ removal kinetics proceeding to completion, and reactivity giving rapid DMT^+ removal. It is likely that the usefulness of triarylsilanes is enhanced by an ability to act also as plasticizers. Triphenyltinhydride is *ca.* 100-fold more reactive than triarylsilanes and used at lower concentrations, in which case any need for increased intrafilm diffusion to abolish microdomains can be met by the inclusion of a plasticizer.

Because DMT^+ scavenging coupled to acid-induced detritylation is irreversible, the use of weaker acids than TCA can be considered, possibly extending the range of useful photoacid generators.

Light sensitivity

Light sensitivity is of considerable practical importance for photodirected array synthesis. It is influenced not only by PAG properties but also the necessary intrafilm acid concentration for extensive detritylation. Our use of a triarylsilane for scavenging achieved >99% detritylation at 60 mJ cm^{-2} (365 nm) within 60 s, a light sensitivity that is 15–100 fold higher than for direct photodeprotection.[26,27] Higher light sensitivities could be achieved

by increasing the post-illumination scavenging period, because the combination of detritylation with scavenging is irreversible. Scavenging is the rate-limiting step: the more reactive the scavenger the faster the detritylation.

Polymeric photoacid generators. The use of enhanced diffusion and its associated movement of photoacid would require careful control to be used in fabrication of very high density arrays with elements of say 4 × 4 μm or less, otherwise photolithographic resolution would be degraded. But a polymeric PAG that on illumination yielded a polymeric acid[28] could overcome this restraint. A co-polymer of styrene and 4-styrene-sulphonic acid esterified with a substituted 2-nitrobenzyl alcohol[29] is an example but the polymeric sulphonium salts described by Kim *et al.*[30] are not, because the photoacid is monomeric.

Diffusion of H^+ or DMT^+ within a solid film of polymeric photoacid could occur by electroneutral hopping of these cations between immobile anionic groups. Illuminated areas lack other mobile anions, non-illuminated areas lack ions of any sort, so diffusion of H^+ from the former areas to the latter would be electrogenic, self-limiting and probably not extending beyond the light/dark boundary by more than a few nm. These circumstances would not be altered by the inclusion of a plasticizer such as TPM to enhance collision rates between surface-attached oligonucleotides and acidic groups on the polymeric photoacid, or between DMT^+ and scavenger molecules.

Conclusion

These concepts and methods for chemical scavenging and the control of intrafilm viscosity within photoacid-generating solid films were developed for the fabrication of oligonucleotide arrays, to pull detritylation to completion rather than force it with strong acid. Novel phosphoramidite building blocks with photolabile protecting groups are not required, and light sensitivity is high. Our own approach may be of wider applicability for the photolithographic miniaturization of chemical syntheses on solid surfaces in cases where a photogenerated compound is a reagent for a reaction that would not proceed to the required degree of completion unless a reaction product within the film is removed either by scavenging or *z*-axis diffusion.

Experimental

Analytical methods

^1H and ^{13}C NMR spectra were recorded using Bruker Avance DPX 600 MHz spectrometer in DMSO-d6 solutions and referenced to the residual DMSO signal. All ^1H and ^{13}C signals are given in ppm (δ scale). The LRMS (LCMS) in ES mode were run using Waters LCT with ESI Lockspray source and Alliance 2795 LC system. GC MS spectra were recorded on ThermoFinnigan Polaris Q instrument. Thin layer chromatography was run on HPTLC (high performance TLC), Merck Kieselgel $60F_{254}$ analytical plates in hexane/EtOAc (9:1) (A). Coarse ICN silica gel was used for short column chromatography.

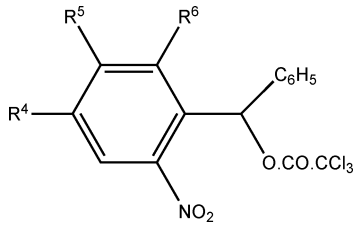

Fig. 8 Structure of trichloroacetic acid photogenerators. We have either described or referred to the synthesis of 25 photosensitive esters of Cl_3CCOOH with variously substituted 2-nitrobenzyl alcohols.[8] Ester **2** ($R^4 = R^5 = OCH_3$, $R^6 = NO_2$) was used for virtually all experiments described here, but mention is made below to ester **1** ($R^4 = R^5 = OCH_3$, $R^6 = H$), ester **6** ($R^4 = H$, $R^5 = Cl$, $R^6 = H$) and ester **7** ($R^4 = H$, $R^5 = Cl$, $R^6 = NO_2$). Each of these four esters formed solid and transparent thin films on glass when cast from DCM solution.

(4-Methoxyphenyl)diphenylsilane

Our synthetic route differs from those previously reported.[31,32] 4-Methoxyphenyl magnesium bromide (1M solution in THF 1.8 mL, 1.8 mmol), was added dropwise by syringe over 10 minutes, at 0–5 °C, under argon, to a solution of diphenylchlorosilane (0.435 g, 1.5 mmol) in THF (6 mL). The resulting mixture was stirred at rt for 16 hours. The mixture was cooled to 0–5 °C and 2% aqueous hydrochloric acid (25 mL) was added dropwise over 20 minutes followed by dichloromethane (50 mL). The organic layer was washed with water (20 mL), 3% aqueous sodium bicarbonate (3 × 20 mL), water (20 mL), brine (20 mL), dried (sodium sulphate) and concentrated in vacuo. The residue was chromatographed on a silica gel column eluting with hexane-ethyl acetate (24:1, v/v) to give the product as a colourless liquid; (0.17 g, 41%); Rf (A) 0.61; ^1H NMR 3.78 (s, 3H, OCH_3), 5.38 (s, 1H, SiH), 7.02 (d, 2H, J= 5.67 Hz, H-3′, H-5′), 7.53 (m, 12H, H-2′, H-6′, 2 x (H-2-H-6)); ^{13}C NMR 54.95 (OCH_3), 114.17 (C-3′, C-5′), 160.86 (C-4′); GC MS for $C_{19}H_{17}OSi$, [M − H], found 289.3.

Bis(4-methoxyphenyl)phenylsilane

4-Methoxyphenyl magnesium bromide (1 M solution in THF 10 mL, 10 mmol), was added dropwise by syringe over 15 minutes, at −10 to 0 °C, under argon, to a solution of dichlorophenylsilane (1.8 g, 1.5 mL, 10 mmol) in THF (6 mL). The resulting mixture was stirred at −10 to 0 °C, under argon, for 2 hours. More 4-methoxyphenyl magnesium bromide (1M solution in THF 10 mL, 10 mmol), was added dropwise by syringe over 15 minutes. The mixture was kept at −10 to 0 °C, for 1 hr and then at rt for 16 hours. The mixture was cooled again to 0 °C, and 2% aqueous hydrochloric acid (50 mL) was added dropwise over 30 minutes followed by dichloromethane (100 mL). The organic layer was washed with water (20 mL), 3% aqueous sodium bicarbonate (3 × 20 mL), water (20 mL), brine (20 mL), dried (sodium sulphate) and concentrated in vacuo. The residue was chromatographed on a silicagel column eluting with hexane-ethyl acetate (95.5:4.5) to give the product as a colourless liquid; (0.99 g, 32%); Rf (A) 0.29; ^1H NMR 3.76 (s, 6H, OCH_3), 5.50 (s, 1H, SiH) 6.97 (d, J = 5.52 Hz, 4H, 2x H-3′, 2x H-5′), 7.43 (m, 9 H, 2x H-2′, 2x H-6′, H-2-H-6); ^{13}C NMR (DMSO-d6) 54.96 (OCH_3), 114.01 (C-3′, C-5′), 161.16 (C-4′); GC MS for $C_{20}H_{19}O_2Si$, $[M - H]^-$, found 319.19; LRMS for $C_{20}H_{20}O_2SiNa$, $[M + Na]^+$, found 342.17.

Attachment of DMT-T to glass slides

We followed literature methods to attach linkers and mononucleotides to glass. Slides derivatized with 3-aminopropyltriethoxysilane were either purchased from Sigma-Aldrich or prepared in our laboratory. We followed literature procedures to prepare (a) 5′-*O*-DMT-thymidine-3′-*O*-succinate by reacting commercially available 5′-*O*-DMT-thymidine with succinic anhydride in the presence of dimethylaminopyridine in dry pyridine, and (b) 5′-*O*-DMT-thymidine-3′-*O*-[(p-nitrophenyl)-succinate] by the condensation of 5′-*O*-DMT-thymidine-3′-*O*-succinate with p-nitrophenol in the presence of dicyclohexylcarbodiimide (DCC) in dioxane.[33] As an alternative glass slides were derivatized with 3-glycidoxypropyltrimethoxysilane followed by ethylene glycol or hexaethylene glycol to provide a terminal primary hydroxyl group.[3] In both preparations we used either whole slides in a staining jar or slides that had been cut into rectangular pieces roughly 20 × 6–7 mm. These pieces can be treated in a round-bottomed flask requiring smaller volumes of reagents.

Coupling of mononucleotides to glass slides derivatized with 3-aminopropyltriethoxysilane

Glass microscope slides, 75 × 25 × 1 mm, were placed in a staining jar and immersed, with stirring, for 120 h at rt in 1 M DCC solution in DCM (45 mL) containing 5′-*O*-DMT-thymidine-3′-*O*-succinate (0.50 g). The slides were then washed thoroughly with dry DMF, dioxane, methanol, acetone, acetonitrile, and diethyl ether and were finally dried *in vacuo* over phosphorus pentoxide overnight. A small fragment (*ca.* 2–3 cm^2) was treated with 1 mL of 3% TCA in DCM (w/v) and the concentration of trityl cation in the resulting solution determined from absorbance measurement at 503 nm. Using commercially available derivatized slides we observed a surface density for 5′-*O*-DMT-thymidine of 50–60 pmol cm^{-2}, and twice that value using slides derivatized in our laboratory.

Coupling of mononucleotides to glass slides derivatized with 3-glycidoxypropyltrimethoxysilane

Rectangular pieces of a derivatized slide were placed in a round bottom flask and treated with 5′-*O*-DMT-thymidine-3′-*O*-phosphoramidite (0.25 g) in dry acetonitrile (5 mL) and activator solution (5 mL of 0.25 M tetrazole in acetonitrile, from Applied Biosystems) added under argon. The reaction was stirred vigorously at rt for 10 minutes and exposed to ultrasound for 5 min. The slides were washed thoroughly with dry acetonitrile and treated with the oxidiser solution (25 mL), from Applied Biosystems, for 60 sec at rt. After being washed again with dry acetonitrile the slides were treated with the Cap A and Cap B solution (1:1 v/v, 25 mL), from Applied Biosystems, and finally washed thoroughly with dry DMF, dioxane, methanol, acetonitrile, acetone, and diethyl ether and dried *in vacuo* over phosphorus pentoxide overnight. A small fragment (2–3 cm^2) was treated with 3% TCA in DCM (1 mL). Absorbance of the resulting solution at 503 nm was used to calculate the loading with 5′-*O*-DMT-thymidine, which was typically 700 pmol cm^{-2} for this method of derivatization.

Film preparation

Thin solid films (*ca.* 0.1–1.5 μm) were cast from DCM solutions onto microscope slides or pieces thereof, as previously described.[8] The presence in the casting solution of some but not all of the tested silanes diminishes the ability of the solutions to wet and spread on a glass surface. This effect became more marked as the concentration or hydrophobicity of the silanes increased. Tri-*n*-butyltinhydride also interfered with film casting. Film-formation was not impaired by triarylsilanes or triphenyltinhydride in film-casting solutions at up to 33% of the solute mass.

Apparatus for photolysis and absorbance measurements of films on glass slides

This was as previously described.[8] However, sensitivity became a major issue when ≥99% detritylation in films left residual DMT-T area densities of ≤2–8 pmol cm^{-2} attached to the underlying glass surface, remaining from pre-detritylation densities of respectively 200–800 pmol cm^{-2}. For these extreme sensitivities we used a deep-well spectrometer with a signal-to-noise ratio in the 480–530 nm region of 2000:1, which with signal averaging reduced the baseline noise to *ca.* ± 0.0005 absorbance units, corresponding to a DMT^+ area density (measured at 510 nm) of ± 0.6 pmol cm^{-2}. This sensitivity was in itself satisfactory, but not if the DMT^+ absorption peak was lost on the side of the much larger peak of the nitroso-photoproduct formed by photolysis of a substituted 2-nitrobenzyl ester (Fig. 8). Amongst such esters[8] the photoproduct of ester **1** gave severe interference, that of ester **2** was satisfactory provided that photolysis was not extensive, and those of esters **6** and **7** gave insignificant interference.

Measurement of photoacid acid production in films

Photolysis of substituted 2-nitrobenzyl esters produces the acid and substituted 2-nitrosobenzophenones. Alternative reaction routes are negligible, and there is a 1:1 stoichiometry between acid release and formation of the 2-nitrosobenzophenone product. The difference spectrum between before and after photolysis is due to the 2-nitrosobenzophenone, and its measurement gives the amount of acid released. For ester **2** the difference spectrum between before and after photolysis in DCM has a peak at 384 nm, with $\varepsilon_{mM} = 4.1$ $mmol^{-1}$ cm^{-1}.

Measurement of film thickness

At the onset of this work we made measurements by interferometry, using the spectrophotometer[8] with a reflectance probe. The intensity of reflected light as a function of wavelength was measured over the range from 400 or 450 nm to 870 nm. Peaks and troughs were observed, their number increasing with film thickness. A glass slide without a film was used as the reference. For calculation of film thickness we used a model with normal incidence of the light beam on the film, and interference between the back reflections from the first and second interfaces, namely air/film and film/glass. The effects of multiple reflections are negligible and can be ignored. But otherwise we obtained the film thickness from the absorbance spectra. The area density (nmol cm^{-2}) of PAG was calculated from the characteristic pre-photolysis UV-absorbance of the PAG. The area density of material (μg cm^{-2})

was then calculated from the PAG density and the casting solution composition, and converted to a film thickness on the assumption that the film density was 1 gm mL^{-1}.

Acknowledgements

This work was supported by grants from the Leverhulme Trust, the BBSRC and EPSRC jointly through Grant No. EGM16064, and the Institute of Cancer Research. We also thank Professor Colin Cooper for his encouragement and support.

References

1 U. Maskos and E. M. Southern, *Nucleic Acids Res*, 1992, **20**, 1679–1684.
2 U. Maskos and E. M. Southern, *Nucleic Acids Res.*, 1993, **21**, 2267–2268.
3 M. H. Caruthers, *Acc. Chem. Res.*, 1991, **24**, 278–284.
4 Abbreviations. BG, Brilliant Green; BGH^+, protonated BG; BMPS, bis(4-methoxyphenyl)phenylsilane; DCM, dichloromethane; DMT, 4.4′-dimethoxytrityl group; DMT^+; 4,4′-dimethoxytrityl carbocation; DMT-T, 5′-*O*-DMT-thymidine; ester **1**, α-phenyl-4,5-dimethoxy-2-nitrobenzyltrichloroacetate; ester **2**, α-phenyl-4,5-dimethoxy-2,6-dinitrobenzyltrichloroacetate; ester **6**, α-phenyl-5-chloro-2-nitrobenzyltrichloroacetate; ester **7**, α-phenyl-5-chloro-2,6-dinitrobenzyltrichloroacetate; MPDPS, 4-(methoxyphenyl)-diphenyl-silane; PAG, photoacid generator; PMS, poly(α-methylstyrene); TCA, trichloroacetic acid; TPM, triphenylmethane; TPS, triphenylsilane; TPTH, triphenyltinhydride.
5 A. C. Pease, D. Solas, E. J. Sullivan, M. T. Cronin, C. P. Holmes and S. P. A. Fodor, *Proc. Natl. Acad. Sci. USA*, 1994, **91**, 5022–5026.
6 G. Wallraff, J. Labadie, P. Brock, R. DiPietro, T. Nyugen, T. Huynh, W. Hinsberg and G. McGall, *CHEMTECH*, 1997, 22–32.
7 J. E. Beecher, G. H. McGall and M. J. Goldberg, *Polym. Mat. Sci. Eng*, 1997, **76**, 597–598.
8 P. J. Serafinowski and P. B. Garland, *Org. Biomol. Chem*, 2008, **6**, 3284–3291.
9 A. B. Sierzchala, D. J. Dellinger, J. R. Betley, T. K. Wyrzykiewicz, C. M. Yamada and M. H. Caruthers, *J. Amer. Chem. Soc.*, 2005, **125**, 13427–13441.
10 M. C. Pirrung, L. Fallon and G. McGall, *J. Org. Chem*, 1998, **63**, 241–246.
11 E. H. Fisher and M. H. Caruthers, *Nucleic Acids Res.*, 1983, **11**, 1589–1599.
12 P. R. Bergethon, E. R. Simons, *E. Biophysical, Chemistry*, (Springer-Verlag, Berlin), 1989, 233-234.
13 B. A. Smith and H. M. McConnell, *Proc. Natl. Acad. Sci. USA*, 1978, **75**, 2759–2763.
14 J. Davoust, P. F. Devaux and L. Leger, *EMBO J*, 1982, **10**, 1233–1238.
15 The ruling consists of evenly spaced parallel opaque chrome lines on clear glass. The line-to-space ratio is unity.
16 Photolysis was at 365 nm for all experiments.
17 We have used polymer preparations of relatively low mol wt, in anticipation that bimolecular reactions in the solid state would be less restrained if intrafilm viscosity is lowered. PMS preparations (Aldrich) were obtained with average M_n values 750 or 1300.
18 Aldrich Chemical Company Polymer Products, CD-Catalog and Reference Guide, 2000, 446–448.
19 C. B. Reese, H. T. Serafinowska and G. Zappia, *Tetrahedron Lett*, 1986, **37**, 2291–2294.
20 V. Ravikumar, M. Andrade, D. Mulvey, D. J. Cole, *US Patent*, 1996, 5,510,476.
21 Polycarbomethylsilane ($CH_3(C_2H_6Si)_nCH_3$)was available at M_{av} values of 800 (mp *ca.* 82 °C) or 2000 (mp > 300 °C). Their films have a slight weakening effect on the ability of photogenerated TCA to detritylate DMT-T incorporated in the film, or to protonate intrafilm BG. This, may be due to bonding of the silyl hydride ($-H^{\delta-}$) with carboxylic hydrogen ($-H^{\delta+}$).
22 N. Wang, J. R. Hwu and E. H. White, *J. Org. Chem.*, 1991, **56**, 471–474; J. B. Lambert, S. Zhang and S. M. Ciro, *Organometallics*, 1994, **13**, 2430–2443.
23 J. L. Duda, J. M. Zielinski, *Diffusion in Polymers*, 1996, Ed. P. Neogi, 143-171. Marcel Dekker Inc, New York.
24 J. E. Beecher, M. J. Goldberg, G. H. McGall, 2000, US Patent 6,083,697.
25 R. G. Kuimelis, G. H. McGall, M. J. Goldberg, G. Xu, 2007, US Patent Application 20070161778.
26 S. Bühler, I. Lagoja, H. Giegrich, K.-P. Stengele and W. Pfleiderer, *Helv. Chim Acta*, 2004, **87**, 620–659.
27 S. P. A. Fodor, J. L. Read, M. C. Pirrung, L. Stryer, A. T. Lu and D. Solas, *Science*, 1991, **251**, 767–773.
28 Throughout this article "acid" refers to Brønsted acid.
29 J. E. Hanson, E. Reichmanis, F. M. Houlihan and T. X. Neenan, *Chem. Mat.*, 1992, **4**, 837–842.
30 M.-H. Kim, D.-Y. Kim, B.-K. Moon, J.-C. Park, Y.-H. Kim, Y.-H., S.-J. Seo, *US Patent* 6,660,479.
31 H. Gilman and G. E. Dunn, *J. Amer. Chem. Soc*, 1951, **73**, 3404–3407.
32 N. Lachance and M. Gallant, *Tetrahedron Lett.*, 1998, **39**, 171–174.
33 T. M. Atkinson, M. Smith, *Oligonucleotide Synthesis: a Practical Approach*. 1984, Ed. M. J. Gait, IRL Press, Oxford & Washington DC, pp. 47–48.